Effect of a symmetry breaking layer on the open circuit voltage of conventional bulk-heterojunction solar cells

Heejoo Kim,[1] Jung Hwa Seo,[2,a)] and Shinuk Cho[3,a)]

[1]*Heeger Center for Advanced Materials and Research Institute for Solar and Sustainable Energies, Gwangju Institute of Science and Technology, Gwangju 500-712, South Korea*
[2]*Department of Materials Physics, Dong-A University, Busan 604-714, South Korea*
[3]*Department of Physics and EHSRC, University of Ulsan, Ulsan 680-749, South Korea*

Solution processable titanium suboxide (TiO_x) was introduced as an artificial symmetry breaking layer in bulk-heterojunction (BHJ) solar cells comprising a low band gap conjugated polymer, poly[(4,4′-bis(2-ethylhexyl)dithiene[3,2-b:2′,3′-d]silole)-2,6-diyl-alt-(4,7-bis(2-thienyl)-2,1,3-benzothiadiazole)-5,5′-diyl] (Si-PCPDTBT), and a soluble fullerene, [6,6]-phenyl-C_{71}-butyric methyl ester ($PC_{71}BM$). The inserted TiO_x layer obviously extracted the same level of open circuit voltage (V_{oc}) regardless of metal work function. Ultraviolet photoelectron spectroscopy (UPS) results indicated that the formation of the interface dipole between the TiO_x symmetry breaking layer and metal electrode successfully modifies the effective work function of the cathode electrode, thereby leading to symmetry breaking in BHJ solar cells. © *2011 American Institute of Physics.* [doi:10.1063/1.3664227]

Bulk-heterojunction (BHJ) solar cells comprising a phase-separated mixture of a semiconducting (conjugated) donor polymer with a soluble fullerene acceptor are of interest as next generation renewable energy sources.[1,2] Recently, as demand for lightweight portable devices increases, power sources for these applications must be lower in cost, thinner, lighter, and mechanically flexible.[3] These demanding features are required to enable paper-like, portable "roll-up" and disposable photovoltaic cells.[4]

In the manufacture of flexible solar cells by printing or roll-to-roll processing, silver (Ag) is the preferred cathode metal because of its solution form processability within roll-to-roll processing.[5–7] However, because Ag has a similar work-function (WF) to indium tin oxide (ITO) (WF of ITO = 4.7 eV, WF of Ag = 4.6 eV), symmetry breaking, which induces an electromotive force for photocurrents, is not spontaneously formed. Consequently, solar cells with Ag electrodes exhibit poor performance due to decreased short circuit current (J_{sc}) and open circuit voltage (V_{oc}).

Symmetry breaking has been emphasized in inverted solar cells. In order to induce sufficient symmetry breaking in inverted solar cells, metal oxide interfacial layers have been introduced between the active layer and the electrodes to modify the WF of electrodes.[8–10] Although this method may be a promising solution in inverted solar cells, several problems should be solved before using this technique in conventional solar cells because there is some difficulty in depositing the metal oxide on the organic layer.

In this study, we have introduced solution processable titanium suboxide (TiO_x) as a symmetry breaking layer in conventional solar cells using a Ag electrode. TiO_x has selective charge transfer properties (hole blocking and electron transferring), thereby artificial symmetry breaking occurs,

allowing for charge extraction.[11–14] In addition, the presence of TiO_x leads to an interfacial dipole at the organic/metal interface that modifies the effective WF of Ag electrodes, thereby enhancing the performance of solar cells fabricated using Ag electrodes. As a result, in BHJ solar cells with Ag electrodes incorporating a TiO_x symmetry breaking layer, almost the same open circuit voltage (V_{oc}) as that of a BHJ solar cell with a low WF metal electrode is achieved (aluminum, Al, WF = 4.2 eV). Our result implies the potential to fabricate high performance BHJ solar cells with Ag "ink" using printing technology in conventional solar cell structures with a TiO_x symmetry breaking layer.

In order to fabricate BHJ solar cells, a low band gap conjugated polymer, poly[(4,4′-bis(2-ethylhexyl)dithiene[3,2-b:2′,3′-d]silole)-2,6-diyl-alt-(4,7-bis(2-thienyl)-2,1,3-benzo-thiadiazole)-5,5′-diyl] (Si-PCPDTBT),[15] and a soluble fullerene, [6,6]-phenyl-C_{71}-butyric methyl ester ($PC_{71}BM$) were used as donor and acceptor materials, respectively. Figure 1(a) shows the schematic diagram of device structures together with chemical structures of the active
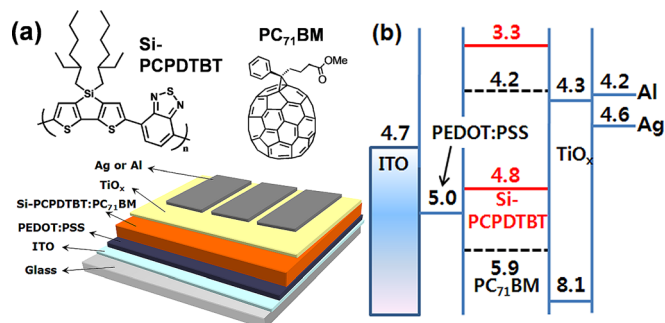

FIG. 1. (Color online) (a) Chemical structures of Si-PCPDTBT and $PC_{71}BM$, and illustration of BHJ solar cell structure. (b) Energy level diagrams of BHJ components including metal electrodes (Al and Ag).

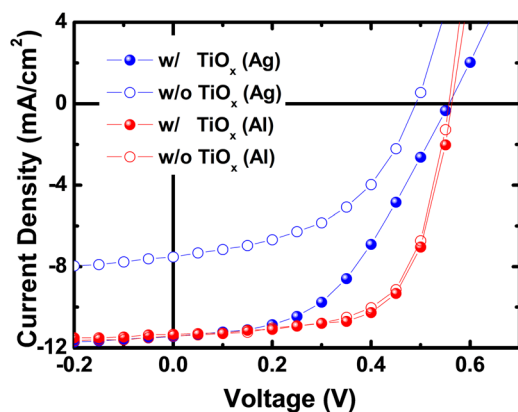a)Authors to whom correspondence should be addressed. Electronic addresses: seojh@dau.ac.kr and sucho@ulsan.ac.kr.

FIG. 2. (Color online) Current density-voltage (J-V) characteristics of Si-PCPDTBT:PC$_{71}$BM BHJ solar cells with and without TiO$_x$ for both Ag and Al electrodes.

TABLE I. Solar cells performance details.

Device		J_{sc} (mA/cm^2)	V_{oc} (V)	FF	PCE (%)
Al	w/o TiO$_x$ (device I)	11.33	0.563	0.658	4.197
	w/TiO$_x$ (device II)	11.42	0.557	0.647	4.113
Ag	w/o TiO$_x$ (device III)	7.53	0.490	0.482	1.778
	w/TiO$_x$ (device IV)	11.44	0.557	0.472	3.008

materials used in this study. Schematic energy level diagrams of each component are also depicted in Fig. 1(b).

BHJ solar cells were fabricated on an ITO-coated glass substrate. Poly(3,4-ethylenedioxylthiophene):poly(styrenesulfonate) (PEDOT:PSS) was spin-cast in air at 5000 rpm for 40 s onto pre-cleaned ITO/glass. The substrate was subsequently dried for 10 min at 140 °C and then transferred into a N$_2$-filled glove box. The blend solution of Si-PCPDTBT:PC$_{71}$BM (1:4 w/w) in 1,2 dichlorobenzene (concentration of 7 mg/1 ml) was spin-cast onto the PEDOT:PSS/ITO/glass (1000 rpm for 60 s). The device was annealed at 80 °C for 10 min in a N$_2$-filled glove box. For devices with a TiO$_x$ layer, as described in detail in earlier publications,[11] the TiO$_x$ solution (diluted by 1:200 in methanol) was spin-cast in air on top of Si-PCPDTBT:PC$_{71}$BM (5000 rpm for 40 s) as the symmetry-breaking and electron extraction layer.[16] The device was heated to 80 °C for 10 min in air. Finally, Al or Ag metal (~100 nm) was deposited by thermal evaporation under high vacuum (4 × 10^{-6} mbar).

Current-voltage (J-V) characteristic curves were measured using a Keithley 236 source measure unit. Solar cell performance was tested using an Air Mass 1.5 Global solar simulator (100 mW/cm^2). An aperture (9.84 mm^2) was used on top of the cell to eliminate extrinsic effects such as cross talk, wave guiding, and shadow effects. External quantum efficiency spectra were measured using a solar cell spectral response/QE/IPCE measurement system (PV measurements Inc. Model QEW 7). All devices were encapsulated with UV epoxy and a cover glass (inside a glove box filled with N$_2$).

For ultraviolet photoelectron spectroscopy (UPS) experiments, 80-nm-thick Ag and Al films were deposited on a pre-cleaned Si substrate with a thin native oxide. A diluted TiO$_x$ (1:200) solution was spin-coated at 4000 rpm for 60 s atop the metal-coated Si substrate. All film preparation was performed in air. Subsequently, films were annealed at 80 °C for 10 min under air. The UPS analysis chamber was equipped with a hemispherical electron energy analyzer (Kratos Ultra Spectrometer) and a UV (He I) source and was maintained at 1 × 10^{-9} Torr. A sample bias of −9 V was used to acquire the high binding energy cutoff. To confirm reproducibility of UPS spectra, we repeated these measurements twice on two sets of samples.

Figure 2 shows the J-V characteristics of Si-PCPDTBT:PC$_{71}$BM solar cells with and without a TiO$_x$ symmetry breaking layer. J-V curves obtained from the solar cells fabricated with Al electrodes are also included for comparison. The solar cell with an Al electrode and without a TiO$_x$ layer (device I) yielded a power conversion efficiency (PCE) of 4.2% with $J_{sc} = 11.33$ mA/cm^2, $V_{oc} = 0.563$ V, and a fill factor (FF) of 0.658. For the solar cell with an Al electrode incorporating the TiO$_x$ layer (device II), a PCE of 4.11% was obtained with $J_{sc} = 11.42$ mA/cm^2, $V_{oc} = 0.557$ V, and $FF = 0.647$. Details related to solar cell performance are listed in Table I. Although the V_{oc} of device II is slightly smaller than that of device II, this can be attributed to the small difference in the lowest unoccupied molecular orbital (LUMO) levels between PC$_{71}$BM and TiO$_x$, as presented in Figure 1(b). Thus, the performances of device I and device II were essentially identical with respect to V_{oc}.

For the solar cell with a Ag electrode and without a TiO$_x$ layer (device III), however, all photovoltaic parameters are significantly decreased. Device III yields a maximum PCE of 1.779% with $J_{sc} = 7.53$ mA/cm^2, $V_{oc} = 0.490$ V, and $FF = 0.482$. A comparison of solar cell characteristics between device III and device IV (with Ag electrode and TiO$_x$ layer) indicates that the insertion of a TiO$_x$ layer yields an increase in both J_{sc} and V_{oc} approaching those obtained using Al electrodes; that is, PCE = 3.008% with $J_{sc} = 11.44$ mA/cm^2, $V_{oc} = 0.557$ V, and $FF = 0.472$. Although the FF
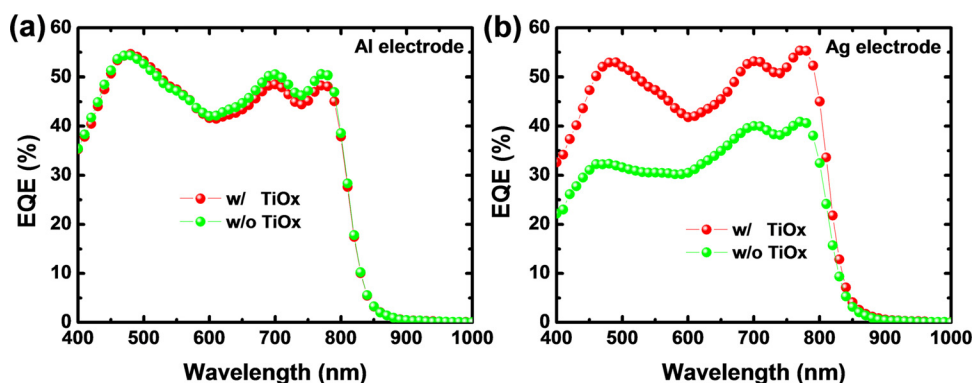

FIG. 3. (Color online) External quantum efficiency spectra for BHJ solar cells fabricated by Si-PCPDTBT:PC$_{71}$BM: (a) with and without TiO$_x$ for Al electrodes and (b) with and without TiO$_x$ for Ag electrode.
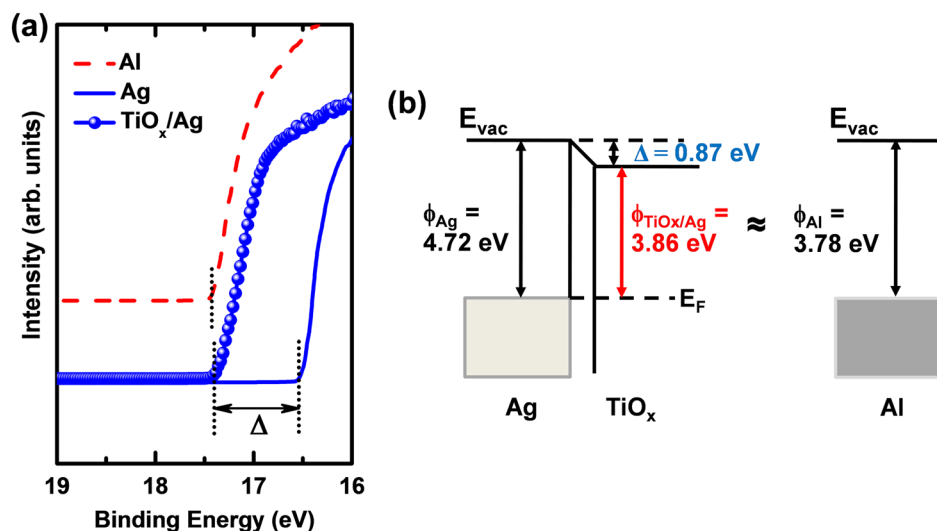
FIG. 4. (Color online) (a) High binding region of normalized UPS spectra of TiO$_x$/Ag films. Al and Ag were used as a reference. (b) Schematic energy levels of TiO$_x$/Ag films with interfacial dipole (Δ). E$_{vac}$: vacuum level, E$_F$: Fermi level, and ϕ = work function.

value of this device is smaller than that of the solar cell with an Al electrode, it is notable that both J_{sc} and V_{oc} in the device with the Ag electrode are almost the same as those of devices I and II.

Figure 3 shows the external quantum efficiency (EQE) spectra for Si-PCPDTBT:PC$_{71}$BM solar cells with and without a TiO$_x$ symmetry breaking layer. For the solar cells with an Al electrode, both EQE spectra of device I and device II are almost identical, which is consistent with J_{sc}, as obtained from the J-V characteristics. The overall EQE spectrum of device III was significantly lower than that of solar cells using an Al electrode. However, the EQE spectrum of solar cells with a TiO$_x$ layer (device IV) increases to the level shown in the solar cells with Al electrodes (device I and device II).

In order to elucidate the modification of the WF of the Ag electrode resulting from the inserted TiO$_x$ layer, UPS measurements were carried out.[14] Figure 4 shows the UPS spectra near the Ag electrode and TiO$_x$/Ag film. Vacuum levels (VLs) of the samples were determined by linear extrapolation of the secondary electron cutoffs on the high binding energy side of the UPS spectra (15–19 eV). The determined work functions for Al and Ag electrodes were 3.78 eV and 4.72 eV, respectively.[16] The onset of UPS spectra (secondary electron cutoffs) of the TiO$_x$/Ag film shifted significantly to a higher binding energy compared to the edge of Ag and showed values similar to those of the Al electrode for secondary electron cutoffs. Because the VL shift indicated the magnitude of the interfacial dipole (Δ),[14,17] the UPS spectra suggest that TiO$_x$/Ag had a strong interfacial dipole (the VL shift of TiO$_x$/Ag was 0.87 eV). The observed values of the interfacial dipole and modified WF of TiO$_x$/Ag are summarized in Figure 3(b). Consequently, we attributed improved solar cell performance of device IV to this reduced WF of Ag by introducing the TiO$_x$ layer.

In conclusion, we have demonstrated the same level of V_{oc} in BHJ solar cells using a mixture of Si-PCPDTBT and PC$_{71}$BM with a high work function metal electrode (Ag) and low work function metal electrode (Al) by incorporating the artificial symmetry breaking TiO$_x$ layer. The TiO$_x$ layer effectively modified the work function of a high work function metal due to interface dipole formation between the active layer and metal electrode; we expect the demonstra-

tion of high performance BHJ solar cells with Ag "ink" using printing technology in conventional solar cell structures with this TiO$_x$ layer in the future.

[1]H. Hoppe and N. S. Sariciftci, J. Mater. Res. **7**, 1924 (2004).
[2]T. D. Nielsen, C. Cruickshank, S. Foged, J. Thorsen, F. C. Krebs, Sol. Energy Mater. Sol. Cells **94**, 1553 (2010)
[3]F. C. Krebs, Sol. Energy Mater. Sol. Cells **93**, 465 (2009).
[4]D. Tobjork and R. Osterbacka, Adv. Mater. **23**, 1935 (2011).
[5]C. Girotto, B. P. Rand, S. Steudel, J. Genoe, and P. Heremans, Org. Electron. **10**, 735 (2009).
[6]Y. Yuan, Y. Bi, and J. Huang, Appl. Phys. Lett. **98**, 063306 (2011).
[7]R. Sondergaard, M. Helgesen, M. Jorgensen, and F. C. Krebs, Adv. Energy Mater. **1**, 68 (2011).
[8]L.-M. Chen, Z. Hong, G. Li, and Y. Yang, Adv. Mater. **21**, 1434 (2009).
[9]T. Ameri, G. Dennler, C. Waldauf, H. Azimi, A. Seemann, K. Forberich, J. Hauch, M. Scharber, K. Hingerl, and C. J. Brabec, Adv. Funct. Mater. **20**, 1592 (2010).
[10]Y. Sun, J. H. Seo, C. J. Takacs, J. Seifter, and A. J. Heeger, Adv. Mater. **23**. 1679 (2011).
[11]J. Y. Kim, S. H. Kim, H.-H. Lee, K. Lee, W. Ma, X. Gong, and A. J. Heeger, Adv. Mater. **18**, 572 (2006).
[12]S. H. Park, A. Roy, S. Beaupré, S. Cho, N. Coates, J. S. Moon, D. Moses, M. Leclerc, K. Lee, and A. J. Heeger, Nat. Photonics **3**, 297 (2010).
[13]J. H. Lee, S. Cho, A. Roy, H-.T. Jung, and A. J. Heeger, Appl. Phys. Lett. **96**, 163303 (2010).
[14]S. Cho, J. H. Seo, K. Lee, and A. J. Heeger, Adv. Funct. Mater. **19**, 1459 (2009).
[15]M. Morana, H. Azimi, G. Dennler, H.-J. Egelhaaf, M. Scharber, K. Forberich, J. Hauch, R. Gaudoana, D. Waller, Z. Zhu et al., Adv. Funct. Mater. **20**, 1180 (2010).
[16]J. H. Seo, R. Yang, J. Z. Brzezinski, B. Walker, G. C. Bazan, and T-.Q. Nguyen, Adv. Mater. **21**. 1006 (2009).
[17]J. H. Seo, A. Gutacker, B. Walker, S. Cho, A. Garcia, R. Yang, T-.Q. Nguyen, A. J. Heeger, and G. C. Bazan, J. Am. Chem. Soc. **131**, 18220 (2009).